

On the Relation between Edge and Vertex Modelling in Shape Analysis

ASGER HOBOLTH

University of Aarhus

JOHN T. KENT

University of Leeds

IAN L. DRYDEN

University of Nottingham

ABSTRACT. Objects in the plane with no obvious landmarks can be described by either vertex transformation vectors or edge transformation vectors. In this paper we provide the relation between the two transformation vectors. Grenander & Miller (1994) use a multivariate normal distribution with a block circulant covariance matrix to model the edge transformation vector. This type of model is also feasible for the vertex transformation vector and in certain cases the free parameters of the two models match up in a simple way. A vertex model and an edge model are applied to a data set of sand particles to explore shape variability.

Key words: circulant symmetry, complex symmetry, deformation, edge transformation, featureless objects, outline, shape, vertex transformation

1. Introduction

Consider a solid object in the plane with no obvious landmarks. Suppose the object can be regarded as a stochastic deformation of a circle. It is often fruitful to describe the object by deforming an n -sided regular polygon using either vertex transformations or edge transformations. In order to describe the variability in shape, it is useful to standardize the edge transformation vector (Kent *et al.*, 2000). A standardized edge transformation vector is invariant under a translation, rotation and isotropic scaling of the object. In this paper we standardize the vertex transformation vectors similarly, and we establish a linear relation between the transformation vectors. An immediate advantage of this unification is that it allows for a comparison of strengths and weaknesses of models independently of whether they are defined as vertex or edge transformation models.

Grenander & Miller (1994) use a multivariate normal distribution to model the edge transformation vector, which is also a feasible model for the vertex transformation vector. The lack of features on the object implies that any statistical model should be invariant under a cyclic permutation of the vertices and this invariance implies that the mean should be zero and that the covariance matrix should be block circulant. To limit the number of free parameters one can propose symmetries or restrictions to the model. We demonstrate how easy it is to go back and forth between the free parameters in the edge and vertex models in some of these cases.

By spacing the vertices in certain ways the data analyst can reduce the dimension of the data from $2n$ to n . This choice of spacing also enables the data analyst to focus on real shape differences rather than differences of the object due to vertex spacing. A vertex and an edge representation of such spacings are presented and in order to compare the two representations we apply them to a data set of sand particles.

Many examples of shape modelling of objects without landmarks can be found in the literature. The objects under study in Grenander & Manbeck (1993), Grenander & Miller (1994), Stoyan & Stoyan (1994, p. 167), Mardia *et al.* (1996), Rue & Syversveen (1998), Hansen *et al.* (2000) and Hobolth & Jensen (2000) are potatoes, mitochondria, sand grains, mushrooms, cells, arteries and cell nuclei, respectively, and they all fall in this category. This list also suggests the wide range of applications of the type of models considered in this paper.

In section 2 the vertex and edge transformation vectors are defined and two simple representations are described. In section 3 the relationship between the transformation vectors is established. In section 4 we describe the model proposed by Grenander & Miller (1994) and in section 5 we consider some special cases of the model where it is easy to go back and forth between the free parameters of a vertex and an edge representation. In section 6 we apply and compare the two simple representations on a data set of sea sand particles collected from a beach at the Baltic Sea.

2. Transformation vectors

In Fig. 1 we show a collection of objects with no obvious landmarks. Furthermore, the objects can be regarded as deformations of a circle. The sample consists of 24 sand grains collected from a beach at the Baltic Sea, as given by Stoyan (1997). In this section we demonstrate how standardized transformation vectors can be used to describe the shape variability of this type of object.

The transformation vectors are defined from a number of vertices collected on the boundary of the object. For arbitrarily chosen vertices, the dimension of the vectors is $2n$, but under certain regular arrangements of the vertices the data analyst can reduce the dimension to n . Examples of such spacings include the radial representation and the constant length representation, which are described in sections 2.1 and 2.2.

2.1. Vertex transformation vectors

Consider an object P in the complex plane with $n \geq 3$ vertices $\tilde{v}_j, j = 0, \dots, n - 1$, located round the outline of the object in an anti-clockwise order. First, make the vertices independent of the location by translating to the new centred vertices

$$v_j = \tilde{v}_j - \frac{1}{n} \sum_{k=0}^{n-1} \tilde{v}_k, \quad j = 0, \dots, n - 1. \tag{1}$$

The sample mean of the vertices is now located at the origin. Let P^0 denote the regular n -sided polygon with vertices

$$v_j^0 = \exp(2\pi i j/n), \quad j = 0, \dots, n - 1. \tag{2}$$

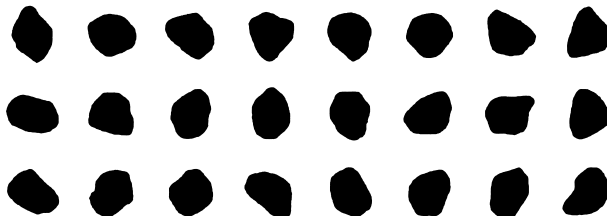


Fig. 1. A sample of 24 sand grains from the Baltic Sea. The sand grains are scaled so that they all have approximately the same area.

The basic idea is to describe the object P as a stochastic deformation of the polygon P^0 . One way of doing this is through a complex-valued “vertex transformation vector” $\mathbf{d} = (d_j)$ defined by

$$d_j = v_j/v_j^0, \quad j = 0, \dots, n - 1. \tag{3}$$

We want to explore the variability in shape and thus we have to investigate the effect of a scaling and rotation of the vertices. Scaling and rotating the vertices by $\alpha \in \mathbb{C}$ leads to

$$\alpha v_j = \alpha d_j v_j^0 = (1 + u_j) v_j^0, \quad j = 0, \dots, n - 1,$$

where

$$u_j = \alpha d_j - 1, \quad j = 0, \dots, n - 1.$$

One possible standardization for α is to rescale and rotate so that

$$u_{av} = \frac{1}{n} \sum_{j=0}^{n-1} u_j = 0, \tag{4}$$

which implies

$$1/\alpha = \frac{1}{n} \sum_{j=0}^{n-1} d_j = d_{av}.$$

Thus, replacing \mathbf{d} by the “standardized vertex transformation vector” $\mathbf{u} = (u_j)$ with components

$$u_j = d_j/d_{av} - 1, \quad j = 0, \dots, n - 1, \tag{5}$$

gives invariance under changes in scale and rotation. The representation in terms of \mathbf{u} breaks down if $d_{av} = 0$, but since $d_{av} = 0$ only for extreme deformations of P^0 this does not pose a practical problem.

The translation (1) implies that

$$\sum_{j=0}^{n-1} v_j = 0,$$

which can be recast in terms of \mathbf{u} as

$$0 = \sum_{j=0}^{n-1} v_j/d_{av} = \sum_{j=0}^{n-1} (1 + u_j) v_j^0 = \sum_{j=0}^{n-1} u_j v_j^0 = \sum_{j=0}^{n-1} u_j \exp(2\pi i j/n), \tag{6}$$

where in the third equality we have used

$$\sum_{j=0}^{n-1} v_j^0 = \sum_{j=0}^{n-1} \exp(2\pi i j/n) = 0.$$

The complex standardization constraint (4) and the complex translation constraint (6) imply that \mathbf{u} has $2n - 4$ free (real) parameters. Note that from

$$v_j = d_{av} (1 + u_j) v_j^0, \quad j = 0, \dots, n - 1,$$

it follows that $\text{Re}(u_j) = r_j$ determines the component of the j th vertex of P tangential to $d_{av} v_j^0$ while $\text{Im}(u_j) = s_j$ determines the normal component.

One often used method of describing a boundary is the radial representation as described below. Let $c \in \mathbb{C}$ be the centre of gravity of the solid two-dimensional object. Find the vertices

of the object by rays starting at c with angles $2\pi j/n, j = 0, \dots, n - 1$, relative to some fixed axis. Suppose the object is star shaped relative to the centre of gravity, i.e. the radial vectors from a single central point to the boundary all remain inside the object. Then the sequence of distances $d_j, j = 0, \dots, n - 1$, provides a description of the boundary. Consider the polygon given by the vertices

$$v_j = d_j v_j^0, \quad d_j \in \mathbb{R}, \quad j = 0, \dots, n - 1.$$

The standardized vertex transformation vector of this polygon is given by

$$u_j = d_j/d_{av} - 1 \in \mathbb{R}, \quad j = 0, \dots, n - 1. \tag{7}$$

Hence, there is variability only in the tangent component $\mathbf{r} = (r_j)$ of the vertex transformation vector, see Fig. 2. Note that in this construction of the vertex transformation vector we avoid centring the vertices as in (1), but take (3) as our starting point. We recommend living with this minor violation of the assumptions since the average of the vertices defined from the centre of gravity is usually close to zero. If the average of the vertices defined from the centre of gravity is not close to zero, then we suggest iterating the construction until a centre is found with the property that the average of the corresponding vertices is close to zero.

There is a large literature on vertex transformation models and usually the radial representation is used. The prior model in Rue & Syversveen (1998) is one example. In a procedure for identifying cells in a digital image, the regular n -sided polygon P^0 is deformed and the generated object is determined by (3), where the vertex transformation vector $\mathbf{d} = (d_j) \in \mathbb{R}^n$ is real and follows a multivariate normal distribution, which is invariant under cyclic permutation. Note that when the components of \mathbf{d} are real and positive then the generated objects are star shaped relative to the origin. Some other examples are given by Rohlf & Archie (1984), Johnson *et al.* (1985), Mardia & Qian (1995) and Mardia *et al.* (1996) who use such representations in modelling mosquito wings, mouse vertebrae, leaves and mushrooms. A description of a Fourier series analysis of radial vector functions is given by Stoyan & Stoyan (1994, p. 80), applied to sand grains. Fourier series analysis has close connections to the analysis of radial vectors, as seen in section 5.4.

2.2. Edge transformation vectors

We now change the focus from the vertices to the edges and recall the standardized edge transformation vector as introduced in Kent *et al.* (2000). Focusing on the edges removes any translation effect immediately. The vector of edges $\mathbf{e} = (e_j)$ for the object P has components

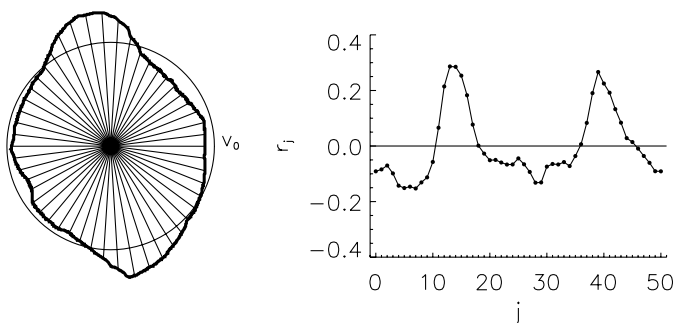


Fig. 2. Left: the rays from the centre of gravity determine the vertices. Right: the value of the tangent component \mathbf{r} of the standardized vertex transformation vector.

$$e_j = v_{j+1} - v_j, \quad j = 0, \dots, n - 1, \tag{8}$$

whereas the vector of edges for the regular polygon P^0 are given by

$$e_j^0 = v_{j+1}^0 - v_j^0 = (\exp(2\pi i/n) - 1)\exp(2\pi i j/n), \quad j = 0, \dots, n - 1.$$

All subscripts throughout the paper are interpreted modulo n . The complex-valued “edge transformation vector” $\mathbf{t} = (t_j)$ can be defined by

$$t_j = e_j/e_j^0, \quad j = 0, \dots, n - 1. \tag{9}$$

Dividing \mathbf{t} by $t_{av} = \sum_{j=0}^{n-1} t_j/n$ gives invariance under changes in scale and rotation and leads to the “standardized edge transformation vector” $\mathbf{z} = (z_j)$ defined by

$$z_j = t_j/t_{av} - 1, \quad j = 0, \dots, n - 1.$$

There are two complex constraints on \mathbf{z} . As in (4) the standardization implies that

$$\frac{1}{n} \sum_{j=0}^{n-1} z_j = z_{av} = 0. \tag{10}$$

Secondly, to ensure that the outline P is closed we also require \mathbf{z} to satisfy

$$0 = \sum_{j=0}^{n-1} e_j/t_{av} = \sum_{j=0}^{n-1} (1 + z_j)e_j^0 = \sum_{j=0}^{n-1} z_j e_j^0 = \sum_{j=0}^{n-1} z_j \exp(2\pi i j/n), \tag{11}$$

and therefore \mathbf{z} has $2n - 4$ free parameters. Note that the constraints on \mathbf{z} and \mathbf{u} are the same. As in the previous subsection it follows from

$$e_j = t_{av}(1 + z_j)e_j^0, \quad j = 0, \dots, n - 1,$$

that $\text{Re}(z_j) = x_j$ determines the component of the j th edge of P tangential to $t_{av}e_j^0$ while $\text{Im}(z_j) = y_j$ determines the normal component.

Another way of collecting vertices on a boundary is that of equal spacing in terms of arc length. If the deformations from a circle are small, the length of each edge remains constant, to first order. This implies that the value of the tangent component \mathbf{x} of the standardized edge transformation vector is zero to first order, and it suffices to consider the normal component \mathbf{y} . In practice, one finds the edge transformation vector $\mathbf{z} = \mathbf{x} + i\mathbf{y}$ of the object and consider $\mathbf{y} = \text{Im}(\mathbf{z})$ as the data, cf. Fig. 3. This way of describing the boundary is called the constant length representation, and is closely related to the tangent angle function, see Zahn & Roskies (1972).

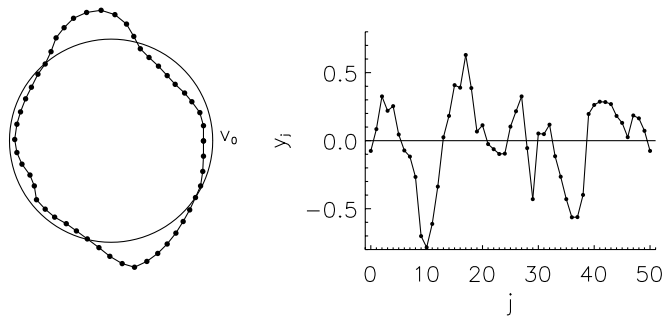


Fig. 3. Left: the vertices are equally spaced in terms of arc length. Right: the value of the normal component \mathbf{y} of the standardized edge transformation vector.

Applications of edge transformation models may be found in Kent *et al.* (2000), where data from sand grains and ceramic material particle sections are analysed, in Grenander & Miller (1994) who describe mitochondria, or in Hansen *et al.* (2000) where images of arteries are considered.

3. The relation between the transformation vectors

We now have two different ways of describing the shape of the object P relative to the regular polygon P^0 , the standardized vertex transformation vector \mathbf{u} and the standardized edge transformation vector \mathbf{z} . The edges are determined by the vertices and, together with a specification of the location, the edges determine the vertices. In this section we show a 1–1 correspondence between the two standardized transformation vectors.

To derive the relationship between the transformation vectors we first note that

$$e_j^0 = (\exp(2\pi i/n) - 1)v_j^0 = (\exp(2\pi i/n) - 1)\exp(-2\pi i/n)v_{j+1}^0.$$

From (3), (8) and (9) it now follows that

$$(\exp(2\pi i/n) - 1)t_j = \exp(2\pi i/n)d_{j+1} - d_j, \quad j = 0, \dots, n - 1,$$

which gives a complex linear relation between \mathbf{t} and \mathbf{d} . The relation implies that $t_{av} = d_{av}$, which shows that the edges and vertices are scaled and rotated in the same way to obtain invariance. Division by $t_{av} = d_{av}$ yields the complex linear relation

$$(\exp(2\pi i/n) - 1)z_j = \exp(2\pi i/n)u_{j+1} - u_j, \quad j = 0, \dots, n - 1, \tag{12}$$

between the standardized vertex transformation vector \mathbf{z} and the standardized edge transformation vector \mathbf{u} . Let B be the circulant $n \times n$ matrix

$$B = \text{circ}(0, 1, 0, \dots, 0).$$

Then (12) can be written as

$$(\exp(2\pi i/n) - 1)\mathbf{z} = (\exp(2\pi i/n)B - I_n)\mathbf{u}. \tag{13}$$

The eigenvalues of B are given by, see Anderson (1971, pp. 280–282),

$$\mu_k = \exp(2\pi i k/n), \quad k = 0, \dots, n - 1,$$

with corresponding unit eigenvectors $\mathbf{w}_k, k = 0, \dots, n - 1$, with components

$$(\mathbf{w}_k)_j = \frac{1}{\sqrt{n}}\exp(2\pi i j k/n), \quad j = 0, \dots, n - 1. \tag{14}$$

Note that \mathbf{w}_k is also an eigenvector for B^T with corresponding eigenvalue $\bar{\mu}_k, k = 0, \dots, n - 1$, where $\bar{\mu}_k$ denotes the complex conjugate of μ_k . The eigenvalues of $(\exp(2\pi i/n)B - I_n)$ are therefore

$$\lambda_k = \mathbf{w}_k^*(\exp(2\pi i/n)B - I_n)\mathbf{w}_k = \exp(2\pi i(k + 1)/n) - 1, \quad k = 0, \dots, n - 1,$$

where $\mathbf{w}_k^* = \bar{\mathbf{w}}_k^T$ is the transposed complex conjugate of \mathbf{w}_k . Since $\lambda_k = 0$ for $k = n - 1$ and $\lambda_k \neq 0$ otherwise the matrix has a singularity corresponding to the eigenvector \mathbf{w}_{n-1} . The constraints (6) and (11) can be written as

$$\mathbf{w}_{n-1}^*\mathbf{z} = \mathbf{w}_{n-1}^*\mathbf{u} = 0,$$

and thus the mapping (13) is 1–1 on the domain of \mathbf{z} and \mathbf{u} . The two other constraints (4) and (10) can be written in terms of the eigenvector \mathbf{w}_0 and thus the 1–1 correspondence between the two standardized transformation vectors follows.

We now recast the relationship between the transformation vectors in terms of real coordinates. Using the equality

$$\tan(\pi/n) = \frac{1 - \cos(2\pi/n)}{\sin(2\pi/n)}$$

it is straightforward to show that

$$\frac{\exp(2\pi i/n)}{\exp(2\pi i/n) - 1} = \frac{1}{2} \left(1 - \frac{i}{\tan(\pi/n)} \right) \quad \text{and} \quad \frac{1}{\exp(2\pi i/n) - 1} = -\frac{1}{2} \left(1 + \frac{i}{\tan(\pi/n)} \right).$$

From (12) it now follows that the relation between the vertex transformation vector \mathbf{u} and the edge transformation vector \mathbf{z} is given by

$$2z_j = \left(1 - \frac{i}{\tan(\pi/n)} \right) u_{j+1} + \left(1 + \frac{i}{\tan(\pi/n)} \right) u_j, \quad j = 0, \dots, n - 1. \tag{15}$$

Letting

$$z_j = x_j + iy_j, \quad u_j = r_j + is_j, \quad j = 0, \dots, n - 1,$$

we can write (15) in real coordinates as

$$2x_j = r_{j+1} + r_j + \frac{1}{\tan(\pi/n)}(s_{j+1} - s_j), \quad j = 0, \dots, n - 1, \tag{16}$$

and

$$2y_j = -\frac{1}{\tan(\pi/n)}(r_{j+1} - r_j) + s_{j+1} + s_j, \quad j = 0, \dots, n - 1. \tag{17}$$

If we let

$$A = \begin{pmatrix} 1 & 1/\tan(\pi/n) \\ -1/\tan(\pi/n) & 1 \end{pmatrix},$$

then the $2n$ equations (16) and (17) can be written as

$$2 \begin{pmatrix} \mathbf{x} \\ \mathbf{y} \end{pmatrix} = (A \otimes B + A^T \otimes I_n) \begin{pmatrix} \mathbf{r} \\ \mathbf{s} \end{pmatrix}, \tag{18}$$

where \otimes denotes the Kronecker product. The basic equations (16) and (17) can also be justified using Fig. 4.

4. A model for the transformation vectors

In this section we consider a multivariate normal model for the standardized vertex transformation vector (\mathbf{r}, \mathbf{s}) . The considerations for a model for the standardized edge transformation vector are similar. To a large extent we follow Kent *et al.* (2000, pp. 529–531), but formulate the results in terms of vertices.

It is convenient to partition the $(2n) \times (2n)$ covariance matrix of (\mathbf{r}, \mathbf{s}) by

$$\text{var} \begin{pmatrix} \mathbf{r} \\ \mathbf{s} \end{pmatrix} = K = \begin{pmatrix} K^{(r,r)} & K^{(r,s)} \\ K^{(s,r)} & K^{(s,s)} \end{pmatrix}.$$

The lack of features on the object implies that any statistical model should be invariant under cyclic permutation of the vertices. Cyclic invariance implies that $E(r_j, s_j)^T = 0$ and

$$E \begin{pmatrix} r_i \\ s_i \end{pmatrix} (r_{i+j}, s_{i+j}) = \begin{pmatrix} a_j & b_j \\ c_j & d_j \end{pmatrix}$$

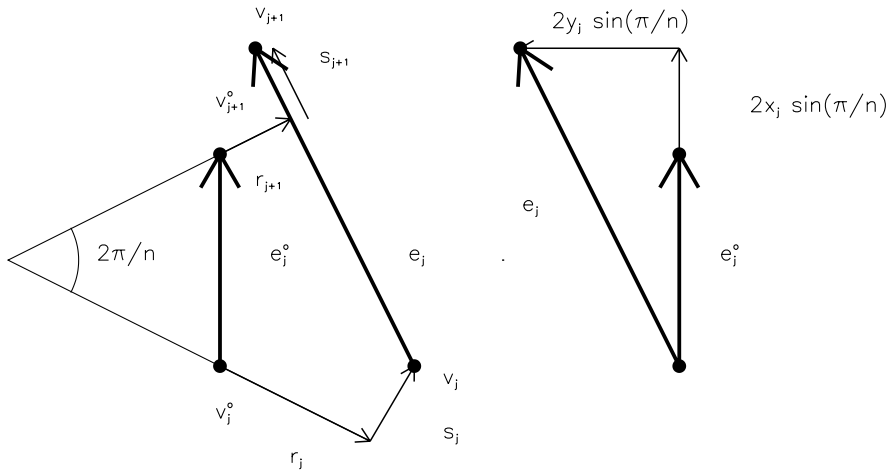


Fig. 4. Illustration of the interpretation of r_j, s_j and x_j, y_j in the case $d_{av} = 1$. The factor $2 \sin(\pi/n)$ comes from the fact that the length of e_j^o is $2 \sin(\pi/n)$. The basic equations (16) and (17) can be found from this figure.

cannot depend on i . Hence there exist numbers $a_j, b_j, c_j, d_j, j = 0, \dots, n - 1$ such that

$$K^{(r,r)} = \text{circ}(a_j), \quad K^{(r,s)} = \text{circ}(b_j), \quad K^{(s,r)} = \text{circ}(c_j), \quad K^{(s,s)} = \text{circ}(d_j),$$

where $\text{circ}(a_j)$ denotes the circulant $n \times n$ matrix with first row (a_0, \dots, a_{n-1}) . The scale and rotation constraint (4) leads to a rank 2 deficiency in K . The translation constraint for the vertices (6) leads to another rank 2 deficiency in K .

Since the four partitioned matrices are all circulant we can make a partial diagonalization of K by the unitary matrix

$$W = (\mathbf{w}_0, \dots, \mathbf{w}_{n-1}), \tag{19}$$

where \mathbf{w}_k is the coloumn vector defined in (14), see Anderson (1971, pp. 280, 281). Let $W^* = \bar{W}^T$ be the transpose of the complex conjugate of W . Then there exist numbers $\alpha_k, \beta_k, \rho_k, \delta_k$ such that,

$$(I_2 \otimes W^*)K(I_2 \otimes W) = \begin{pmatrix} \text{diag}(\alpha_k) & \text{diag}(\beta_k) \\ \text{diag}(\rho_k) & \text{diag}(\delta_k) \end{pmatrix} = D, \tag{20}$$

where $\text{diag}(\alpha_k)$ denotes the diagonal $n \times n$ matrix with $\alpha_0, \dots, \alpha_{n-1}$ on the main diagonal.

By diagonalizing the blocks

$$D(k) = \begin{pmatrix} \alpha_k & \beta_k \\ \rho_k & \delta_k \end{pmatrix}$$

one can obtain a complete diagonalization of K . Denote the eigenvalues of $D(k)$ by $\kappa_{1,k}$ and $\kappa_{2,k}$ and write the eigenvectors in the form

$$\gamma_{1,k} = \begin{pmatrix} \cos \theta_k \\ \exp(i(\phi_k - \pi/2)) \sin \theta_k \end{pmatrix}, \quad \gamma_{2,k} = \begin{pmatrix} -\sin \theta_k \\ \exp i(\phi_k - \pi/2) \cos \theta_k \end{pmatrix}, \quad 0 \leq \theta_k, \phi_k < \pi,$$

for suitable choices of θ_k and ϕ_k . It then follows that $\gamma_{m,k} \otimes \mathbf{w}_k$ is an eigenvector of K for $\kappa_{m,k}, m = 1, 2$. The conditions on $\{a_j, b_j, c_j, d_j\}$ imply conditions on $\{\alpha_k, \beta_k, \rho_k, \delta_k\}$, which can

also be expressed as conditions on $\{\kappa_{m,k}, \theta_k, \phi_k\}$. It turns out that for $1 \leq k < n/2$, $D(k)$ and $D(n-k)$ have the same eigenvalues $\kappa_{m,k}, m = 1, 2$ with eigenvectors $\gamma_{m,k}, m = 1, 2$ and $\bar{\gamma}_{m,k}, m = 1, 2$, respectively. Together with $\mathbf{w}_k = \bar{\mathbf{w}}_{n-k}$ this implies that $\kappa_{m,k}, m = 1, 2$ has multiplicity 2 for $1 \leq k < n/2$. Furthermore, the standardization constraint (4) implies that the eigenvalues for $k = 0$ must vanish, $\kappa_{1,0} = \kappa_{2,0} = 0$. Similarly, the translation constraint (6) implies that for $k = 1$ the first eigenvalue must vanish, $\kappa_{1,1} = 0$.

In total, the eigenvalues and eigenvectors of $D(k)$ satisfy the following conditions:

- $k = 0$: $\kappa_{1,0} = \kappa_{2,0} = 0$;
 θ_0, ϕ_0 irrelevant.
- $k = 1$: $\kappa_{1,1} = 0, \kappa_{2,1} \geq 0$ a free parameter;
 $\theta_1 = 3\pi/4, \phi_1 = 0$.
- $1 < k < n/2$: $\kappa_{m,k} \geq 0, m = 1, 2$, free parameters;
 $\theta_k \in [0, \pi], \phi_k \in [0, \pi]$ free parameters.
- $k = n/2, (n \text{ even})$: $\kappa_{m,n/2} \geq 0, m = 1, 2$, free parameters;
 $\theta_{n/2} \in [0, \pi]$ a free parameter; $\phi_{n/2} = \pi/2$.

Let

$$\begin{pmatrix} \mathbf{r} \\ \mathbf{s} \end{pmatrix} \sim N_{2n}(0, K).$$

With $R = A \otimes B + A^T \otimes I_n$ it follows from (18) that

$$\begin{pmatrix} \mathbf{x} \\ \mathbf{y} \end{pmatrix} \sim N_{2n}\left(0, \frac{1}{4} RKR^T\right).$$

In general, the free parameters $\{\kappa_{m,k}, \theta_k, \phi_k\}$ for K do not match up in a simple way with the free parameters in a similar diagonalization of $RKR^T/4$.

5. Special cases

To limit the number of free parameters one can propose symmetries or restrictions to the model. In this section we consider such cases. We demonstrate how easy it is to go back and forth between the free parameters of the edge and the vertex model in the complex symmetric case and in the radial representation. The eigenvalues are often restricted through a Markov random field (MRF) model. We show that a first-order MRF model for the edges implies a second-order MRF model for the vertices in the complex symmetric and in the radial representations.

5.1. Complex symmetry

A complex Gaussian random vector $\mathbf{u} = \mathbf{r} + i\mathbf{s}$ with mean $\mathbf{0}$ is said to possess complex symmetry if

$$E(r_{j_1} r_{j_2}) = E(s_{j_1} s_{j_2}), \quad E(r_{j_1} s_{j_2}) = -E(s_{j_1} r_{j_2}), \quad 0 \leq j_1, j_2 \leq n - 1.$$

This property implies that \mathbf{u} and $\exp(i\theta)\mathbf{u}$ have the same distribution for any θ . If \mathbf{u} possesses complex symmetry then from (16) and (17) it is straightforward to show that $\mathbf{z} = \mathbf{x} + i\mathbf{y}$ also possesses complex symmetry. In the complex symmetric case it can be shown, see Kent *et al.* (2000, p. 532), that the blocks of $D(k)$ take the form

$$D(k) = \begin{pmatrix} \alpha_k & i\beta_k \\ -i\beta_k & \alpha_k \end{pmatrix}, \quad 1 \leq k < [n/2],$$

where $\alpha_k \geq 0, \beta_k \in \mathbb{R}, -\alpha_k \leq \beta_k \leq \alpha_k$ and $\beta_{n/2} = 0$ (n even). Thus, the eigenvalues of $D(k)$ are $\alpha_k \pm \beta_k$ with corresponding unit eigenvectors

$$\mathbf{q}_1 = \frac{1}{\sqrt{2}} \begin{pmatrix} 1 \\ i \end{pmatrix} \quad \text{and} \quad \mathbf{q}_2 = \bar{\mathbf{q}}_1.$$

In this case the blocks of D can be expressed in the following parameters:

$$\begin{aligned} k = 0 : & \quad \kappa_{1,0} = \kappa_{2,0} = 0; \\ & \quad \theta_0, \phi_0 \text{ irrelevant.} \\ k = 1 : & \quad \kappa_{1,1} = 0, \kappa_{2,1} \geq 0 \text{ a free parameter;} \\ & \quad \theta_1 = 3\pi/4, \phi_1 = 0. \\ 1 < k < n/2 : & \quad \kappa_{m,k} \geq 0, m = 1, 2 \text{ free parameters;} \\ & \quad \theta_k = \pi/4, \phi_k = 0. \\ k = n/2, (n \text{ even}) : & \quad \kappa_{m,n/2} \geq 0, m = 1, 2 \text{ free parameters;} \\ & \quad \theta_{n/2} = 0, \phi_{n/2} = \pi/2. \end{aligned}$$

Hence, the complex symmetric model is determined by the sequence of eigenvalues $\kappa_{1,k}$ and $\kappa_{2,k}$. The covariance matrix of \mathbf{u} and the covariance matrix of \mathbf{z} have the same eigenvectors and the eigenvalues $\kappa_{m,k}^u$ and $\kappa_{m,k}^z$ are related by the following proposition.

Proposition 1

In the complex symmetric model the free eigenvalues for the vertex transformation vector $\kappa_{m,k}^u$ and the free eigenvalues for the edge transformation vector $\kappa_{m,k}^z$ are related by

$$\kappa_{1,k}^z = g_1(k)\kappa_{1,k}^u, \quad 2 \leq k \leq [n/2],$$

and

$$\kappa_{2,k}^z = g_2(k)\kappa_{2,k}^u, \quad 1 \leq k \leq [n/2],$$

where

$$g_1(k) = \frac{1}{2} \left(1 + \frac{1}{\tan(\pi/n)^2} \right) + \frac{1}{2} \left(1 - \frac{1}{\tan(\pi/n)^2} \right) \cos(2\pi k/n) - \frac{\sin(2\pi k/n)}{\tan(\pi/n)},$$

and

$$g_2(k) = \frac{1}{2} \left(1 + \frac{1}{\tan(\pi/n)^2} \right) + \frac{1}{2} \left(1 - \frac{1}{\tan(\pi/n)^2} \right) \cos(2\pi k/n) + \frac{\sin(2\pi k/n)}{\tan(\pi/n)}.$$

Proof. First note that \mathbf{q}_1 and \mathbf{q}_2 are also eigenvectors of A (defined in (18)) with corresponding eigenvalues

$$\omega_1 = 1 + i/\tan(\pi/n) \quad \text{and} \quad \omega_2 = \bar{\omega}_1.$$

The proposition now follows from a direct calculation since

$$\begin{aligned} \kappa_{1,k}^z &= (\mathbf{q}_1 \otimes \mathbf{w}_k)^* \frac{1}{4} RKR^T (\mathbf{q}_1 \otimes \mathbf{w}_k) \\ &= \frac{1}{4} (\mathbf{q}_1 \otimes \mathbf{w}_k)^* (A \otimes B + A^T \otimes I_n) K (A^T \otimes B^T + A \otimes I_n) (\mathbf{q}_1 \otimes \mathbf{w}_k) \\ &= \frac{1}{4} (\omega_1 \mu_k + \bar{\omega}_1) (\bar{\omega}_1 \bar{\mu}_k + \omega_1) (\mathbf{q}_1 \otimes \mathbf{w}_k)^* K (\mathbf{q}_1 \otimes \mathbf{w}_k) \\ &= g_1(k)\kappa_{1,k}^u, \quad 2 \leq k \leq [n/2]. \end{aligned}$$

The relation between $\kappa_{2,k}^z$ and $\kappa_{2,k}^u$ is shown in a similar way. An alternative proof can be based on the complex representation (4.3). The quantities $g_1(k)$ and $g_2(k)$ appear as the squared absolute eigenvalues of $(\exp(2\pi i/n)B - I_n)/(\exp(2\pi i/n) - 1)$ for the eigenvectors \mathbf{w}_{n-k} and \mathbf{w}_k , respectively.

Note that g_1 and g_2 are non-linear and largely monotonic (except near $k = n/2$). For large n and small k the relationship is approximately quadratic, as $g_1(k) \approx (k - 1)^2$ and $g_2(k) \approx (k + 1)^2$; see Fig. 5.

The complex symmetric model is a rather restrictive model since it forces the tangential and normal components $r_j, s_j (x_j, y_j)$ of the standardized vertex (edge) transformation vector to have the same variance and to be uncorrelated.

5.2. Complex symmetry with a MRF structure

One way to impose further structure on the eigenvalues is through a p th-order Markov random field (MRF) model. The complex form of this model for an n -vector \mathbf{u} takes the form

$$E\mathbf{u} = \mathbf{0}, \quad E\mathbf{u}\mathbf{u}^* = 2\Sigma,$$

where $\Sigma^{-1} = (\sigma^{jk})$ is banded with non-zero entries

$$\sigma^{j,j+l} = \bar{\sigma}^{j+l,j} = \alpha_l, \quad l = 0, \dots, p.$$

Here $\alpha_0 > 0$ and $\alpha_1, \dots, \alpha_p$ are allowed to be complex. The eigenvalues η_k^u of this circulant covariance matrix are given by

$$1/\eta_k^u = \alpha_0 + 2 \sum_{l=1}^p \text{Re}(\alpha_l \exp(2\pi ikl/n)), \quad k = 0, \dots, n - 1.$$

In the terminology of section 4, $\kappa_{1,k} = \eta_{n-k}^u, \kappa_{2,k} = \eta_k^u$. The α_l parameters must be chosen to ensure the eigenvalues are positive in order to guarantee a positive definite covariance matrix. A sufficient condition is $2 \sum_{l=1}^p |\alpha_l| < \alpha_0$.

We now describe how to include the constraints (4) and (6), or equivalently (10) and (11). Let

$$\Sigma = W^* \text{diag}\{\eta_k^u\}W$$

be the spectral decomposition of a complex covariance matrix satisfying the MRF assumption. Then the covariance matrix

$$W^* \text{diag}\{0, \eta_0^u, \dots, \eta_{n-2}^u, 0\}W$$

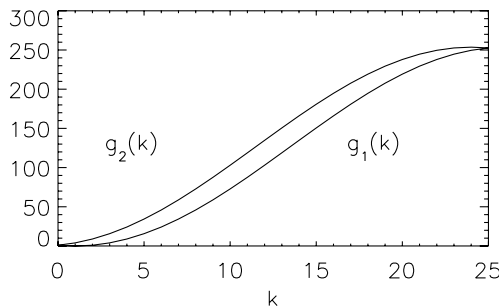


Fig. 5. Plot of $g_1(k)$ and $g_2(k)$ for $n = 50$.

with the eigenvalues for $k = 0, n - 1$ replaced by 0 satisfies the required constraints. Note that the parameter space for the α_l parameters is larger in the constrained model since fewer eigenvalues are required to be positive.

Consider for simplicity the complex symmetric first-order MRF model for the edge transformation vector \mathbf{z} given by

$$\alpha_0 = 1/\sigma^2, \quad \alpha_1 = -\beta/(2\sigma^2),$$

and subject to the constraints (10) and (11). A sufficient condition for positive definiteness for the covariance matrix is

$$\sigma^2 > 0, \quad \beta \in \mathbb{C} \quad \text{and} \quad |\beta| < 1,$$

but note that this parameter space can be enlarged as just described.

Proposition 2

The constrained complex symmetric first-order MRF model for the edge transformation vector \mathbf{z} corresponds to a constrained complex symmetric second-order MRF model for the vertex transformation vector \mathbf{u} given by

$$\alpha_0 = \left\{ 2 \left(1 + \frac{1}{\tan(\pi/n)^2} \right) - \left(1 - \frac{1}{\tan(\pi/n)^2} \right) \text{Re}(\beta) + 2 \frac{\text{Im}(\beta)}{\tan(\pi/n)} \right\} / (4\sigma^2)$$

$$\alpha_1 = \left\{ \left(1 - \frac{i}{\tan(\pi/n)} \right)^2 - \left(1 + \frac{1}{\tan(\pi/n)^2} \right) \beta \right\} / (4\sigma^2)$$

$$\alpha_2 = \left\{ -\frac{1}{2} \left(1 - \frac{i}{\tan(\pi/n)} \right)^2 \beta \right\} / (4\sigma^2).$$

Proof. In terms of \mathbf{z} and \mathbf{u} we can write (15) as

$$2\mathbf{z} = \left(1 - \frac{i}{\tan(\pi/n)} \right) B\mathbf{u} + \left(1 + \frac{i}{\tan(\pi/n)} \right) \mathbf{u},$$

and the proposition follows from the change of variables formula. Another way to prove proposition 2 is to use the real version of the model and apply the relationship between the eigenvalues established in proposition 1.

Thus, a conditioned first-order MRF model for the edge transformation vector is equivalent to a conditioned second-order MRF model for the vertex transformation vector. Note that in general a p th-order MRF model for the edge transformation vector corresponds to a $(p + 1)$ th-order MRF model for the vertex transformation vector. A similar result can be found in Kent *et al.* (1996).

An application of the complex symmetric edge transformation model is given by Hurn *et al.* (1999) who use the model as the prior for one type of cell. The complex symmetric edge transformation model has a MRF structure with $\beta \in \mathbb{R}$, and their model incorporates a constraint for closure, but not for size and rotation.

5.3. *The radial representation*

Suppose there is variability only in the radial component \mathbf{r} of the vertex transformation vector $\mathbf{u} = \mathbf{r} + i\mathbf{s}$ and no variability in the normal component \mathbf{s} . This restriction leads to zero entries

in K apart from $K^{(r,r)}$. Denote the eigenvalues of the covariance matrix $K^{(r,r)}$ by κ_k^r with corresponding eigenvectors $\mathbf{w}_k, k = 0, \dots, n - 1$. Similarly, let κ_k^x and κ_k^y denote the eigenvalues of the covariance matrix of the tangent component \mathbf{x} and the normal component \mathbf{y} of the edge transformation vector $\mathbf{z} = \mathbf{x} + i\mathbf{y}$.

Proposition 3

In the radial representation the free eigenvalues of the tangent component of the vertex transformation vector, κ_k^x , and the free eigenvalues of the tangent and normal component of the edge transformation vector, κ_k^x and κ_k^y , respectively, are related by

$$\kappa_k^x = \frac{1}{2}(1 + \cos(2\pi k/n))\kappa_k^r, \quad k = 0, \dots, n - 1,$$

and

$$\kappa_k^y = \frac{1 - \cos(2\pi k/n)}{2 \tan(\pi/n)^2} \kappa_k^r, \quad k = 0, \dots, n - 1. \tag{21}$$

Proof. Since there is no variability in the normal component of the vertex transformation vector $\mathbf{s} = \mathbf{0}$, and we get from (16) that

$$2\mathbf{x} = (B + I)\mathbf{r}. \tag{22}$$

A direct calculation gives

$$\begin{aligned} \kappa_k^x &= \mathbf{w}_k^* K^{(x,x)} \mathbf{w}_k = \frac{1}{4} \mathbf{w}_k^* (B + I) K^{(r,r)} (B^T + I) \mathbf{w}_k \\ &= \frac{1}{4} (\mu_k + 1)(\bar{\mu}_k + 1) \mathbf{w}_k^* K^{(r,r)} \mathbf{w}_k \\ &= \frac{1}{2} (1 + \cos(2\pi k/n)) \kappa_k^r, \quad k = 0, \dots, n - 1. \end{aligned}$$

From (17) we have that

$$2\mathbf{y} = -\frac{1}{\tan(\pi/n)} (B - I)\mathbf{r}, \tag{23}$$

and (21) follows from a similar calculation.

Note that for large n and small k we have $\kappa_k^x \approx \kappa_k^r$ and $\kappa_k^y \approx k^2 \kappa_k^r$. The major part of the variability from a circle is described by the eigenvectors with small and large k . Thus, in the radial representation with many landmarks the large part of the variability from a circle is in the normal direction of the edge transformation vector.

5.4. The radial representation with a MRF structure

The real form of a p th-order model for an n -vector \mathbf{r} takes the form

$$\mathbf{E}\mathbf{r} = \mathbf{0}, \quad \mathbf{E}\mathbf{r}\mathbf{r}^T = \Sigma,$$

where $\Sigma^{-1} = \sigma^{jk}$ is banded with non-zero entries

$$\sigma^{j,j+l} = \sigma^{j+l,j} = \alpha_l, \quad l = 0, \dots, p.$$

Here $\alpha_0 > 0$ and $\alpha_1, \dots, \alpha_p$ are real and chosen to ensure the eigenvalues

$$\kappa_k = 1/(\alpha_0 + 2 \sum_{l=1}^p \alpha_l \cos(2\pi kl/n))$$

of the covariance matrix are positive.

A periodic stationary stochastic process can be derived by letting $n \rightarrow \infty$ and letting the α_l vary with n . The limiting process is most simply described as a random Fourier series

$$r(t) = \sum_{k \in \mathbb{Z}} \left\{ \zeta_k^c \left(\kappa_k^{(\infty)} \right)^{1/2} \cos(2\pi kt) + \zeta_k^s \left(\kappa_k^{(\infty)} \right)^{1/2} \sin(2\pi kt) \right\},$$

where the ζ_k^c, ζ_k^s are i.i.d. $N(0, 1)$ random variables and the eigenvalues take the form

$$1/\kappa_k^{(\infty)} = a_0 + \sum_{l=1}^p a_l (2\pi k)^{2l},$$

and the a_l are real. If this process is restricted to the equally-spaced points $t = 2\pi j/n, j = 0, \dots, n - 1$, for some value of n , then a circulant random vector results, with eigenvalues $\kappa_k^{(C)}$, say, given by

$$1/\kappa_k^{(C)} = \sum_{m \in \mathbb{Z}} 1/\kappa_{k+nm}^{(\infty)},$$

after taking aliasing into account.

Consider the radial model with no variability in the normal component of the vertex transformation vector. The relation between \mathbf{y} and \mathbf{r} is then given by (23). The constraints on \mathbf{r} are

$$\sum_{j=0}^{n-1} r_j = \sum_{j=0}^{n-1} r_j \cos(2\pi j/n) = \sum_{j=0}^{n-1} r_j \sin(2\pi j/n) = 0,$$

and these constraints can be recast in terms of \mathbf{y} as

$$\sum_{j=0}^{n-1} y_j = \sum_{j=0}^{n-1} y_j \cos(2\pi j/n) = \sum_{j=0}^{n-1} y_j \sin(2\pi j/n) = 0.$$

As in the complex symmetric case the constraints are most simply implemented in the spectral domain where they correspond to setting $\kappa_0^r = \kappa_1^r = \kappa_{n-1}^r = 0$.

For simplicity let the model for the normal component of the edge transformation vector be a first-order MRF model given by

$$\alpha_0 = 1/\sigma^2, \quad \alpha_1 = -\beta/(2\sigma^2),$$

with the sufficient condition

$$\sigma^2 > 0, \quad \beta \in \mathbb{R} \quad \text{and} \quad |\beta| < 1,$$

for positive definiteness for the covariance matrix.

Proposition 4

The constrained radial first-order MRF model for the normal component of the edge transformation vector corresponds to a constrained second-order MRF model for the tangent component of the vertex transformation vector given by

$$\alpha_0 = c(2 + \beta), \quad \alpha_1 = -c(1 + \beta), \quad \alpha_2 = c\beta/2,$$

where $1/c = 4\sigma^2 \tan(\pi/n)^2$.

Proof. From proposition 3 it follows that

$$\begin{aligned}
 1/\kappa_k^r &= \frac{1 - \cos(2\pi k/n)}{2 \tan(\pi/n)^2} \frac{1}{\kappa_k^y} \\
 &= \frac{2 + \beta - (1 + \beta)2 \cos(2\pi k/n) + \beta \cos(4\pi k/n)}{4\sigma^2 \tan(\pi/n)^2} \\
 &= \frac{1}{4\sigma^2 \tan(\pi/n)^2} \mathbf{w}_k^* \left((2 + \beta)L_n - (1 + \beta)(B + B^T) + \frac{\beta}{2}(B^2 + (B^T)^2) \right) \mathbf{w}_k, \\
 & \quad k = 2, \dots, n - 2.
 \end{aligned}$$

The proposition can also be shown directly from (23) and the change of variables formula.

6. Data analysis

6.1. Data representation and model specification

For arbitrarily spaced vertices around the outline of an object, the full normal models for the edge and vertex representations are interchangeable. However, in practice the data analyst can often choose the spacing of the vertices. Choosing the vertices to be regularly spaced, or the edges to have constant length, leads to a more succinct description of the data. In sections 2.1 and 2.2 we discussed the radial and the constant length representations. They both have the advantage of reducing the dimension of the data from $2n$ to n without losing any important information.

Consider the radial representation. Since there is no variability in the normal component \mathbf{s} of the standardized vertex transformation vector we have zero entries in K apart from $K^{(r,r)}$. As in the previous section denote the eigenvalues of $K^{(r,r)}$ by κ_k^r with corresponding eigenvectors $\mathbf{w}_k, k = 0, \dots, n - 1$. Since $K^{(r,r)}$ is symmetric and circulant and $\mathbf{w}_k = \bar{\mathbf{w}}_{n-k}$ we have $\kappa_k^r = \kappa_{n-k}^r, k = 1, \dots, [n/2]$. Therefore we only have to consider $\kappa_0^r, \dots, \kappa_{[n/2]}^r$. The constraints (4) and (6) imply $\kappa_0^r = \kappa_1^r = \kappa_{n-1}^r = 0$. The considerations for the constant length representation are similar. For the constant length representation there is no variability in the radial component \mathbf{x} of the standardized edge transformation vector, and thus we only have to consider the normal component \mathbf{y} , which is modelled by the symmetric and circulant covariance matrix $K^{(y,y)}$ with the same constraints.

To impose further structure on the eigenvalues we consider a real version of the p th-order continuous MRF model discretized to n points as described in section 5.4. The general p th-order model has $p + 1$ parameters, but from exploratory fits we found that in our application a two parameter p th-order model with $a_1 = \dots = a_{p-1} = 0$ is sufficiently flexible. Thus, the free eigenvalues are given by

$$\kappa_k^r = \sum_{m \in \mathbb{Z}} \frac{1}{\alpha + \beta \{2\pi(k + nm)\}^{2p}}, \quad 2 \leq k \leq [n/2]. \tag{24}$$

The continuous two parameter first-order model with $p = 1$ was considered in Kent *et al.* (2000) and the continuous two parameter second-order model with $p = 2$ was considered in Hobolth & Jensen (2000), although without taking aliasing into account (i.e. only the term with $m = 0$ is present). The parameter space is given by

$$\beta > 0, \quad \alpha > -(4\pi)^{2p} \beta,$$

to ensure that the eigenvalues are positive. The parameters α, β determine the overall shape variability. The parameter β in (24) determines how fast the eigenvalues are decreasing and can

be viewed as a smoothness parameter. The parameter α is mainly important for the first few eigenvalues and therefore reflects global shape variability.

It is often useful to consider the marginal likelihoods for the first few eigenvalues only. Following Kent *et al.* (2000) we shall label the model $Full(k^*)$ when we ignore the eigenvalues with indices greater than k^* , where k^* satisfies $2 \leq k^* \leq [n/2]$. Similarly the two parameter model with eigenvalues given by (24) is labelled two parameter $CMRF(p, k^*)$ when we ignore the eigenvalues with indices greater than k^* .

6.2. Statistical inference

Next we consider statistical inference for some of the radial models. Inference in the full normal model of section 4 may be found in Kent *et al.* (2000). Consider a random sample of N standardized vertex transformation vectors from the radial representation

$$\mathbf{r}_l = (r_{l,0}, r_{l,1}, \dots, r_{l,n-1})^T, \quad l = 1, \dots, N,$$

drawn independently from the multivariate normal model

$$\mathbf{r}_l \sim N(\mathbf{0}, K^{(r,r)}), \quad l = 1, \dots, N,$$

where $K^{(r,r)}$ is a symmetric, circulant $n \times n$ matrix with the constraints $\kappa_0^r = \kappa_1^r = \kappa_{n-1}^r = 0$. The maximum likelihood estimator (MLE) of $K^{(r,r)}$ is given by

$$\hat{K}^{(r,r)} = \frac{1}{Nn} \sum_{l=1}^N \sum_{p=0}^{n-1} \mathbf{r}_l^{(p)} (\mathbf{r}_l^{(p)})^T,$$

where $\mathbf{r}_l^{(p)}$ denotes \mathbf{r}_l cyclically permuted by p sites, i.e.

$$\mathbf{r}_l^{(p)} = (r_{l,p}, r_{l,1+p}, \dots, r_{l,n-1+p})^T,$$

and the sample eigenvalues are

$$\hat{\kappa}_k^r = \mathbf{w}_k^* \hat{K}^{(r,r)} \mathbf{w}_k, \quad k = 0, \dots, n-1.$$

Ignoring the components κ_0^r and $\kappa_1^r = \kappa_{n-1}^r$ and using $\kappa_k^r = \kappa_{n-k}^r, k = 2, \dots, [n/2]$, the marginal likelihood becomes

$$\left(\prod_{k=2}^{[n/2]} 2\pi(\kappa_k^r)^{\tau_k} \right)^{-N/2} \exp\left(-\frac{N}{2} \sum_{k=2}^{[n/2]} \tau_k \frac{\hat{\kappa}_k^r}{\kappa_k^r} \right), \tag{25}$$

where $\tau_k = 2, 1 \leq k < [n/2]$, and $\tau_{n/2} = 1$, the last term being present only for n even. Thus, under the radial representation the MLEs of the parameters $\kappa_k^r, k = 2, \dots, [n/2]$ are the sample eigenvalues $\hat{\kappa}_k^r, k = 2, \dots, [n/2]$.

The likelihood for the more restricted two parameter $CMRF(p, k^*)$ is given by (25) with $[n/2]$ replaced by k^* and κ_k^r given by (24). To calculate the MLEs of (α, β) we use numerical maximization of the log-likelihood.

Testing if the two parameter $CMRF(p, k^*)$ is a reasonable simplification of the $Full(k^*)$ is carried out using a classical likelihood ratio test. Let L_1 be the maximized likelihood under the $Full(k^*)$ with $v_1 = k^* - 1$ free parameters and L_2 the maximized likelihood under the two parameter $CMRF(p, k^*)$ with $v_2 = 2$ free parameters. For a large sample size N we have the χ^2 approximation

$$-2 \log(L_2/L_1) \simeq \chi_{(v_1-v_2)}^2.$$

6.3. Application

We consider inference for the parameters in the models using the sand particle data for illustration. For each of the N sand grains we first determine the vector

$$\mathbf{r}_l = (r_{l,0}, r_{l,1}, \dots, r_{l,n-1})^T, \quad l = 1, \dots, N,$$

using the radial representation described in section 2.1. Each sand grain is represented by a binary image (1 for an object grey level and 0 for a background grey level). The centre of gravity of the image is obtained, and then equally spaced radii are traced out to the boundary. A boundary point is defined as the pixel location before the first zero is obtained. The number of vertices n on each outline should be chosen high enough to capture the shape of the object, but since the objects are only represented as binary images not much extra information is gained by choosing a very high n . We have chosen the rather high $n = 50$.

Now consider the constraints. From $\sum_{j=0}^{n-1} r_j = 0$ it follows that $\hat{\kappa}_0^r = 0$. If the sample mean of the vertices is zero then we get from (6) that $\hat{\kappa}_1^r = \hat{\kappa}_{n-1}^r = 0$. In practice the sample mean of the vertices is only approximately zero and hence $\hat{\kappa}_1^r = \hat{\kappa}_{n-1}^r$ is only approximately zero.

In order to avoid the effect of digitization it is useful to consider only the first few well-determined eigenvalues. The choice of the truncation value k^* is based on the eigenvalues, which should be truncated when they are essentially determined by noise due to digitization effects. We choose $k^* = 10$. Note that when k^* is small compared to $[n/2]$ then the specific choice of n is less important. The sample log-eigenvalues $\log \hat{\kappa}_k^r$ are shown in Fig. 6 for $k = 2, \dots, k^*$.

A two parameter $CMRF(2, 10)$ is fitted to the data and the MLEs are $(\hat{\alpha}, \hat{\beta}) = (1.108, 0.000120)$. To see whether the two parameter $CMRF(2, 10)$ is reasonable the likelihood ratio test is carried out. We obtain $-2 \log(L_2/L_1) = 4.34$ and accept the MRF model on $v_1 - v_2 = 7$ degrees of freedom, the p -value being 0.74. In Fig. 6 we have plotted the log-eigenvalues under the fitted two parameter $CMRF(2, 10)$ model. Similarly one can fit a two parameter $CMRF(1, 10)$ or a two parameter $CMRF(3, 10)$ to the data and it turns out that neither of these models is appropriate.

A similar analysis as for the radial vertex representation was carried out for the constant length edge representation. For each of the N sand grains we first determine the vector

$$\mathbf{y}_l = (y_{l,0}, \dots, y_{l,n-1})^T, \quad l = 0, \dots, N,$$

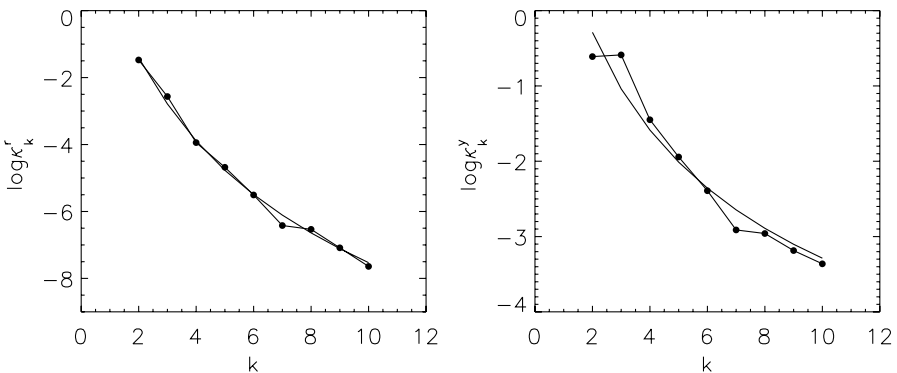


Fig. 6. Plot of the logarithm of the eigenvalues under the $Full(10)$ (line with filled points) and under the two parameter $CMRF(p, 10)$ (line without points) for the radial ($p = 2$, left) and constant length ($p = 1$, right) representations.

as described in section 2.2. As before we denote the eigenvalues of $K^{(y,y)}$ by κ_k^y . The constraints are as in the radial representation. From (10) it follows that $\hat{\kappa}_0^y = 0$. Furthermore, since (11) holds approximately with z_j replaced by y_j we have $\hat{\kappa}_1^y = \hat{\kappa}_{n-1}^y \approx 0$. The two parameter $CMRF(p, 10)$ is then fitted to the data. In this case it turns out that the first-order model with $p = 1$ is appropriate and the MLEs are $(\hat{\alpha}, \hat{\beta}) = (0.125, 0.0077)$. When we test the two parameter $CMRF(1, 10)$ against the $Full(10)$ we obtain the likelihood ratio $-2\log(L_2/L_1) = 10.56$ and accept the two parameter $CMRF(1, 10)$ on 7 degrees of freedom, the p -value being 0.16. In Fig. 6 we have plotted the fitted log-eigenvalues under the full model and under the first-order MRF model. Bearing the results from section 5 in mind it should be no surprise that a first-order MRF model for an edge model “corresponds” to a second-order MRF model for a vertex model.

An effective way of examining a model is to inspect random samples from the model. In Fig. 7 we have simulated outlines from the fitted MRF models. The outlines from the radial and constant length representations look like realistic sea sand grains. Furthermore the simulated samples from the two representations look very much alike. The simulated outlines are a little smoother than the sand grains, but this was expected because of the truncation. From the simulations it seems that both models are adequate for the sea sand grains.

In comparing the two methods it does seem that in this particular application the radial vertex representation follows the second-order MRF model more closely than the constant length edge representation follows the first-order MRF model (although both are deemed reasonable fits from the tests). The radial vertex representation also has the advantage that in general it is easier to construct the discrete data from a continuous outline, although the representation is restricted to star shaped objects.

6.4. Recommendation

The shape of objects in the plane with no obvious landmarks can be described by a variety of different methods. In this paper we have concentrated on an approach based on the standardized edge or vertex transformation vector. When deciding which model to use for the transformation vector one has to take into account how the vertices have been collected. If there is variability in both the real and imaginary part of the transformation vector, then the full normal model described in section 4 is needed. This model has the required circulant symmetries, but is also rather complicated with many $(2n - 4)$ free parameters. One way of imposing constraints on the free parameters is through the more restrictive complex symmetric or even complex symmetric Markov random field models. The complex linear 1–1 relation between the standardized transformation vectors makes it possible to recast any edge model in terms of a vertex model and vice versa. In the general model the free parameters do not match up in a simple way, but in the complex symmetric models there is a simple correspondence as described in proposition 1 and proposition 2 of section 5. See Table 1 for a summary of the possible representations and models when the vertices are arbitrarily spaced.

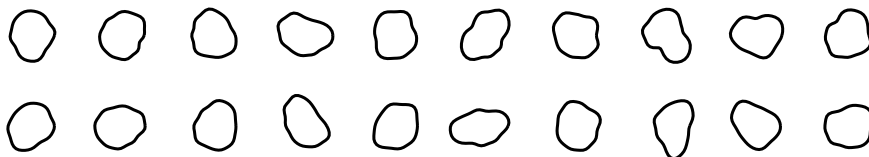


Fig. 7. Simulated objects under the fitted MRF models. The first row shows simulations from the radial second-order MRF model and the second row is from the constant length first-order MRF model.

Table 1. Summarizing the possible representations and models when the vertices are arbitrarily spaced

Representation	Data	Models		
vertex	$\mathbf{u} = \mathbf{r} + i\mathbf{s}$	General (section 4)	Complex symm. (section 5.1)	Complex symm. MRF (section 5.2)
edge	$\mathbf{z} = \mathbf{x} + i\mathbf{y}$			

Table 2. Summarizing the possible representations and models when the vertices are regularly spaced or the edges have constant length

Representation	Data	Models		
Radial vertex	\mathbf{r}	Full(k^*) (section 6.1)	CMRF(p, k^*) (sections 5.4 and 6.1)	two parameter CMRF(p, k^*) (section 6.1)
Constant length edge	\mathbf{y}			

Choosing the vertices to be regularly spaced, or the edges to have constant length, leads to a more succinct description of the data than when the vertices are arbitrarily spaced. The radial and the constant length representations have the advantage of reducing the dimension of the data from $2n$ to n without losing any important information, and furthermore they allow the data analyst to focus on honest differences rather than differences due to the vertex spacing. Unfortunately the vertex spacing is different in the two representations so a direct comparison of the full radial model and the full constant length model is not possible. Instead of the full models we might again impose restrictions on the eigenvalues of the covariance matrix through Markov random field models. For the sand grains the radial representation follows a MRF model more closely than the constant length representation, but this outcome would have been hard to predict. If the vertex spacing can be decided by the data analyst then we suggest analysing both the radial and the constant length model before deciding on a final model. See Table 2 for a summary of the possible representations and models when the vertices are regularly spaced or the edges have constant length.

Acknowledgements

The first author thanks Eva B. Vedel Jensen for fruitful discussions. The authors wish to thank Dietrich Stoyan for kindly providing the sand particle data and an associate editor and two referees for constructive suggestions leading to a better presentation of the contents of the paper.

References

- Anderson, T. W. (1971). *The statistical analysis of time series*. Wiley, New York.
- Grenander, U. & Manbeck, K. M. (1993). A stochastic model for defect detection in potatoes. *J. Comput. Graph. Statist.* **2**, 131–151.
- Grenander, U. & Miller, M. I. (1994). Representations of knowledge in complex systems (with discussion). *J. Roy. Statist. Soc. Ser. B* **56**, 549–603.
- Hansen, M. B., Møller, J. & Tøgersen, F. Aa. (2000). Bayesian contour detection in a time series of ultrasound images through dynamic deformable template models. Research Report 17, Centre for Mathematical Physics and Stochastics, University of Aarhus. To appear in *Biostatistics*.
- Hobolth, A. & Jensen, E. V. B. (2000). Modelling stochastic changes in curve shape, with an application to cancer diagnostics. *Adv. Appl. Probab. (SGSA)* **32**, 344–362.
- Hurn, M. A., Steinsland, I. & Rue, H. (1999). Parameter estimation for a deformable template model. Statistics Research Report 99.02, University of Bath. To appear in *Statist. Comput.*

- Johnson, D. R., O'Higgins, P., McAndrew, T. J., Adams, L. M. & Flinn, R. M. (1985). Measurement of biological shape: a general method applied to mouse vertebrae. *J. Embryol. Exper. Morphol.* **90**, 363–377.
- Kent, J. T., Mardia, K. V. & Walder, A. N. (1996). Conditional cyclic Markov random fields. *Adv. Appl. Probab. (SGSA)* **28**, 1–12.
- Kent, J. T., Dryden, I. L. & Anderson, C. R. (2000). Using circulant symmetry to model featureless objects. *Biometrika* **87**, 527–544.
- Mardia, K. V. & Qian, W. (1995). Bayesian method for compact object recognition from noisy images. In *Complex stochastic systems in science and engineering* (ed. D. M. Titterton), 155–165, Clarendon Press, Oxford.
- Mardia, K. V., Qian, W., Shah, D. & De Souza, K. (1996). Deformable template recognition of multiple occluded objects. *IEEE Trans. Pattern Anal. Machine Intell.* **19**, 1036–1042.
- Rohlf, F. J. & Archie, J. (1984). A comparison of Fourier methods for the description of wing shape in mosquitoes. *Systematic Zool.* **33**, 302–317.
- Rue, H. & Syversveen, A. R. (1998). Bayesian object recognition with Baddeley's Delta Loss. *Adv. Appl. Probab. (SGSA)* **30**, 64–84.
- Stoyan, D. (1997). Geometrical means, medians and variances for samples of particles. *Particle Systems Characterization* **14**, 30–34.
- Stoyan, D. & Stoyan, H. (1994). *Fractals, random shapes and point fields: methods of geometric statistics*. Wiley, Chichester.
- Zahn, C. T. & Roskies, R. Z. (1972). Fourier descriptors for plane closed curves. *IEEE Trans. Comput.* **C-21**, 269–281.

Received June 2000, in final form August 2001

Asger Hobolth, Department of Mathematical Sciences, University of Aarhus, Ny Munkegade, DK-8000 Aarhus C, Denmark.
E-mail: asho@imf.au.dk